

An Assessment of Soil Metal Contamination in Oil Fields Utilizing Petroleum Contamination Indices and GIS Methods

Khaldoon T. Falih ^{a*}

^{a} Civil Techniques Department, Nasiriyah Technical Institute, Southern Technical University, Baghdad Street, Nasiriyah 64001, Iraq. E-mail: khaldoon.talib@stu.edu.iq*

Abstract

In recent decades, there has been a growing focus on soil quality due to the significant industrialization and urbanization observed in many places worldwide. The primary hazards to soil are recognized as a reduction in organic material, heightened soil erosion. The metal content of samples collected from March to August at ten different stations in the Al-Garraff Oil Field was analysed (Cd, Cr, Cu, Fe, Mn, Ni, Pb, and Zn). The correlation analysis revealed that organic matter from petroleum waste affected the metal content of the Al-Garraff Oil Field. The values found in the literature have been compared to the results. Using the geoaccumulation index (I_{geo}) to calculate the metal pollution status in the oil field The results of the I_{geo} index reveal that the soil of Al-Garraff Oil Field was moderately contaminated with heavy metals (Cd, extremely contaminated by Mn, and heavily to heavily extremely contaminated by Pb metal. The correlation matrix reveals a significant positive association between Cr-Mn, Cu-Pb, Cu-Ni, Zn-Cu, and Zn-Pb, indicating that these heavy metals have a same origin. An inverted distance weighted (IDW) technique in GIS was utilised to generate and analyse a map of heavy metal concentrations for the purpose of illustrating the pollutant distribution in a lucid fashion. The map visually represented the stations most significantly impacted by these elements.

Keywords: Heavy Metal. Al-Garraff Oil Field, Geoaccumulation Index. GIS, Inverse Distance Weighted (IDW).

Introduction

Globally, scientists and environmentalists are presently embarking on an endeavour to surmount the obstacle of eradicating the deleterious consequences of soil, air, and water contamination. Significant sources of petroleum contamination in our environment include extensive crude oil spills onto soil, pipeline leaks, underground and surface fuel storage tank leaks, indiscriminate spills, negligent waste disposal and mismanagement of waste and other petroleum by-products generated by society, among others. Because of its cancer-causing, mutation-causing, and poisonous properties, it has emerged as a subject of discussion and garnered an increasing amount of attention [16, 13, 3].

Utilizing the geographical information system (GIS) to gather, display, and analyse topographically relevant data is invaluable. By integrating geostatistical methods with GIS, soil scientists are able to manage extensive databases that are utilised for the mapping of various soil property types [6, 1]. IDW (Inverse Distance Weight) is a deterministic method of interpolation that operates using inverse distance weighting. The distance-reversed function of each point from its neighbors characterizes it, under the assumption that the rate of correlations and similarities between neighboring points is proportional to their distance from one another [14, 15]. Although attempts have been made to identify the most appropriate method, inverse distance weighting (IDW) has been extensively implemented to forecast the regional variability of soil parameters in industrial activities [12, 1].

A study of the distribution, enrichment, accumulation of heavy and contamination factor metals in soils of the oil fields is particularly important, especially in developing countries like Iraq due to the unprofessional and lawless manner in which are dealt with industries and petroleum waste.

An improved method of evaluating the hazards linked to released petroleum waste involves the examination of metal distribution in soil in close proximity to residential and agricultural zones. This analysis furnishes empirical support for the industry's influence on ecosystems. The goal of this research was to identify whether or not potentially harmful heavy metal concentrations were present in the soil immediately surrounding the site under investigation [16, 11]. Heavy metals of concern were Cd, Cr, Cu, Fe, Mn, Ni, Pb, and Zn. The consideration of four aspects: (1) Monthly and regional distribution of the metals in the soil, (2) Producing a foundational repository for future studies to draw from in Garraf Oil field (3) Determining if there is any evidence of metals in the soil came from Al-Garraf Oil Field, and (4) determining geoaccumulation index and create maps for heavy metals using IDW methods in GIS.

Case Study

The Garraf Oil Field is situated in the southern part of Iraq, in Thi-Qar Governorate fig. 1. The oil field was first discovered in 1984. The oil field, with a width of 5.5 km and average length of 17.5 km. The Gharraf oil field is vital to the southern Iraqi region. After recent improvements to the field's infrastructure, this field's production capacity has reached (170,000) Barrel.

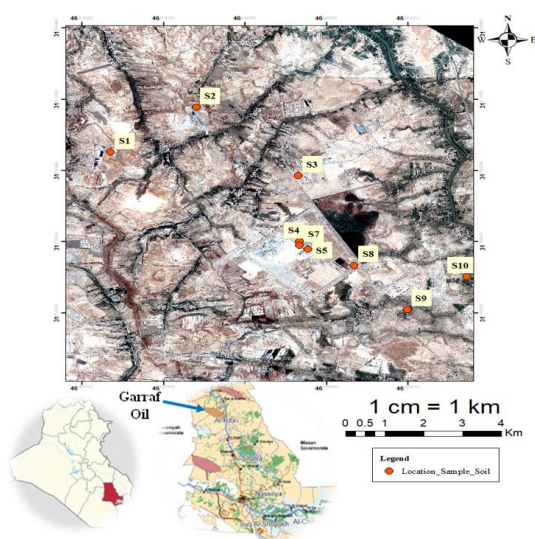


Fig. 1: Geographic Location and Distribution of Some Sampling Sites in the Gharraf Oil Field

Sampling and Sample Preparation

Soil samples were taken monthly for ten sites (S-1, S-2, S-3, S-4, S-5, S-6, S-7, S-8, S-9, and S-10) in the Al-Gharraf oil field. We collected samples for six months (August, July, June, May, April, and March 2022). We used the USEPA-3050A method in the laboratory to prepare these samples. We use this technique, known as acid digestion, to process sediments, sludges, and soil samples for analysis using flame or furnace atomic absorption spectroscopy (FLAA and GFAA, respectively), or inductively coupled argon plasma spectroscopy (ICP). The preparation process was as follows: We use nitric acid and hydrogen peroxide to break down a representative sample weighing between 1 and 2 grammes (wet weight). After that, the digestate goes through a reflux process with either nitric or hydrochloric acid. Both flame AA and ICP analyses require the use of hydrochloric acid, while furnace AA work requires the application of nitric acid. We use diluted hydrochloric acid as the final reflux acid for the ICP analysis of As and Se, and for the flame AA or ICP analysis of Cd, Cr, Cu, Fe, Mn, Ni, Pb, and Zn. Nitric acid, which has been diluted, is used as the final dilution acid in the furnace AA analysis of Cd, Cr, Fe, and the diluted samples have an acid concentration of approximately 5.0 percent (v/v). For the determination of the total percentage of solids, a separate sample needs to be dried, [10, 9].

Methods

Cadmium (Cd) mg/kg

Monthly variations of Cadmium (Cd) mg/kg were observed during this study. The highest month concentrations (4.260 mg/kg) were detected during August month, while the lowest month concentration (0 mg/kg) was noticed during March month (Table 1, Fig. 2).

Table 1: Monthly Variations of (Cd) mg/kg in the Soil with Mean in Al-Garraf Oil Field

Locations	S-1	S-2	S-3	S-4	S-5	S-6	S-7	S-8	S-9	S-10
Month 2022										
March	0.105	0.17	0.104	0.104	0.103	0.105	0.105	0.108	0.108	0.114
April	0.177	0.175	0.174	0.171	0.168	0.166	0.178	0.182	0.166	0.177
May	0.192	0.19	0.189	0.186	0.183	0.181	0.193	0.197	0.181	0.192
June	0.212	0.21	0.209	0.206	0.203	0.201	0.213	0.217	0.201	0.212
July	0.222	0.28	0.238	0.216	0.213	0.211	0.233	0.227	0.211	0.222
August	0.231	0.294	0.247	0.225	0.222	0.22	0.248	0.236	0.22	0.231
Mean	0.190	0.220	0.194	0.185	0.182	0.181	0.195	0.195	0.181	0.191

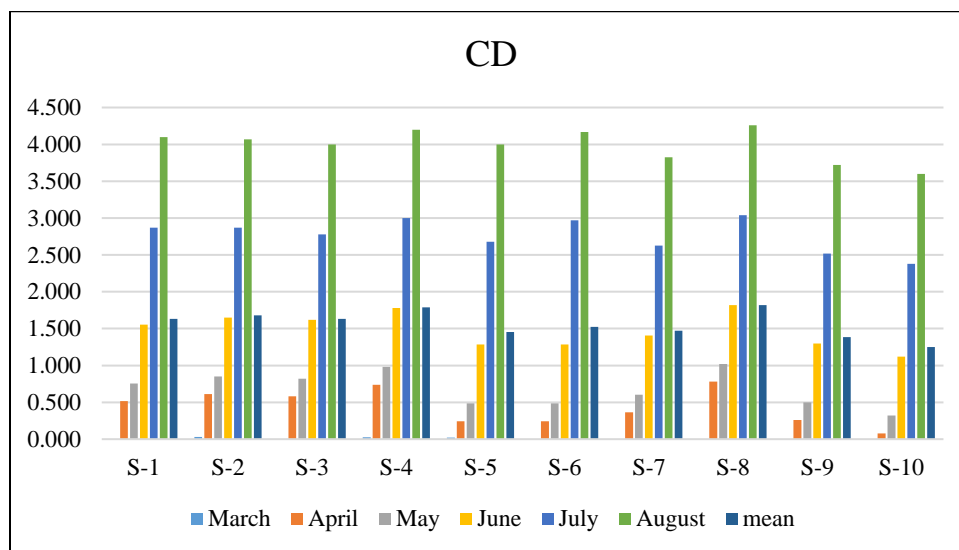


Fig. 2: Monthly Concentrations of (Cd) mg/kg at Al-Garraf Oil Field

Chromium (Cr)

Monthly variations of Chromium (Cr) mg/kg were observed during this study. The highest month concentrations (394.900 mg/kg) detected during August month, while lowest month concentration (29.800 mg/kg) noticed during April month (Table 2, Fig. 3).

Table 2: Monthly Variations of (Cr) mg/kg in the Soil with Mean in Al-Garraff Oil Field

Locations Month 2022	S-1	S-2	S-3	S-4	S-5	S-6	S-7	S-8	S-9	S-10
March	49.066	48.804	65.140	48.823	97.671	81.926	65.567	73.778	72.877	73.705
April	110.300	99.000	44.200	110.700	112.600	106.200	81.500	107.000	29.800	98.800
May	121.420	110.120	55.320	121.820	123.720	117.320	92.620	118.120	40.920	109.920
June	331.920	320.620	265.820	369.320	365.220	327.820	303.120	330.620	251.420	320.420
July	347.200	335.900	281.110	384.200	380.500	343.590	318.400	345.900	265.870	335.700
August	357.600	346.400	291.610	394.900	391.000	355.000	328.900	356.400	276.370	347.000
Mean	219.584	210.141	167.200	238.294	245.119	221.976	198.351	221.970	156.210	214.258

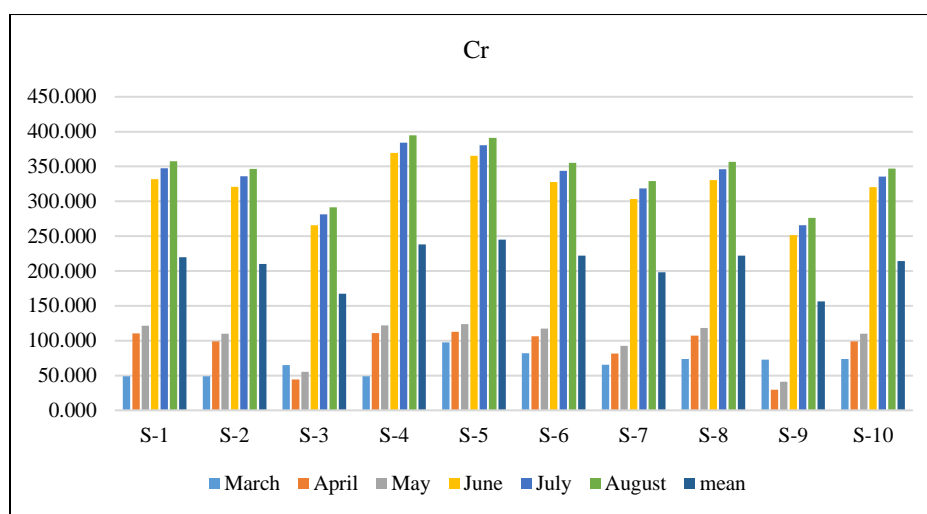


Fig. 3: Monthly Concentrations of (Cr) mg/kg at Al-Garraff Oil Field

Copper (Cu)

Monthly variations of Copper (Cu) mg/kg were observed during this study. The highest month concentrations (200 mg/kg) detected during August month, while lowest month concentration (0 mg/kg) noticed during April month (Table 3, Fig. 4).

Table 3: Monthly Variations of (Cu) mg/kg in the Soil with Mean in Al-Garraff Oil Field

Locations Month 2022	S-1	S-2	S-3	S-4	S-5	S-6	S-7	S-8	S-9	S-10
March	46.210	27.120	20.800	29.980	19.290	25.480	20.850	35.370	32.830	15.460
April	34.923	24.611	20.637	29.024	nil	23.715	20.241	35.162	149.016	26.170
May	38.164	27.852	23.878	32.265	2.251	26.956	23.482	38.403	152.257	29.411
June	68.415	58.103	54.129	62.516	32.502	57.207	53.733	68.654	182.508	59.662
July	78.695	68.383	65.410	72.796	41.988	67.487	64.013	78.958	192.788	69.942
August	85.254	74.603	71.630	80.100	48.208	74.200	70.233	85.178	200.000	76.162
Mean	58.610	46.779	42.747	51.114	28.848	45.841	42.092	56.954	151.567	46.135

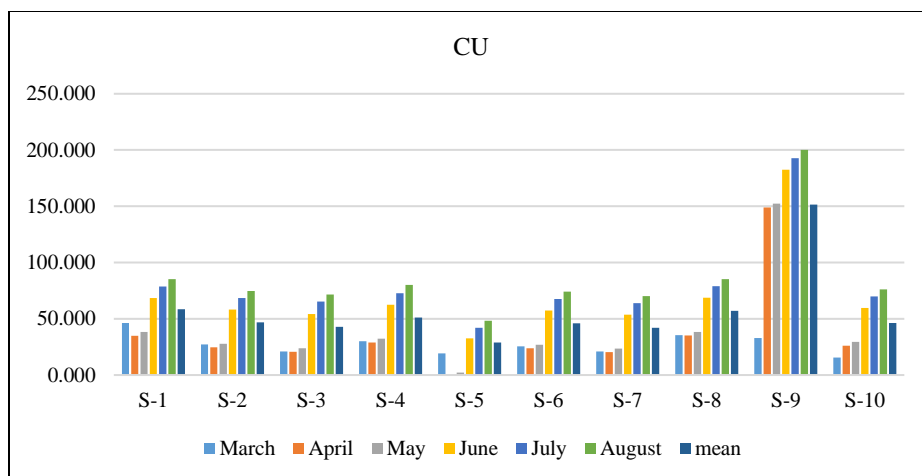


Fig. 4: Monthly Concentrations of (Cu) mg/kg at Al-Garraff Oil Field

Manganese (Mn)

Monthly variations of Manganese (Mn) mg/kg were observed during this study. The highest month concentrations (355.6 mg/kg) detected during August month, while lowest month concentration (211.4 mg/kg) noticed during March month (Table 4, Fig. 5).

Table 4: Monthly Variations of (Mn) mg/kg in the Soil with Mean in Al-Garraff Oil Field

Locations Month 2022	S-1	S-2	S-3	S-4	S-5	S-6	S-7	S-8	S-9	S-10
March	276.500	294.600	211.400	301.800	315.600	306.600	297.800	288.600	211.800	225.300
April	276.500	294.600	211.400	301.800	315.600	306.600	297.800	288.600	211.800	225.300
May	279.750	297.850	214.650	305.050	318.850	309.850	301.050	291.850	215.050	228.550
June	295.000	314.200	230.200	320.300	334.500	325.100	315.200	307.100	230.300	243.600
July	305.250	325.050	242.150	330.550	345.000	335.350	325.450	317.350	241.250	253.850
August	318.100	335.650	253.000	341.150	355.600	350.200	336.050	327.950	251.850	265.000
Mean	291.850	310.325	227.133	316.775	330.858	322.283	312.225	303.575	227.008	240.267

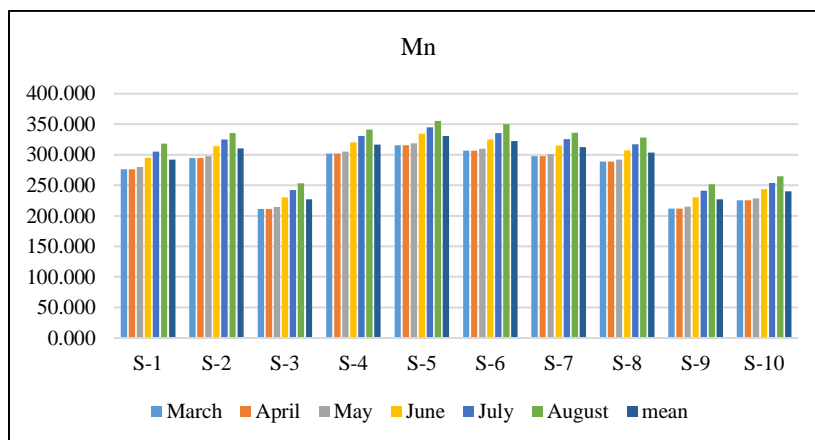


Fig. 5: Monthly Concentrations of (Mn) mg/kg at Al-Garraff Oil Field

Lead (Pb)

Monthly variations of Lead (Pb) mg/kg were observed during this study. The highest month concentrations (1064.34 mg/kg) detected during August month, while lowest month concentration (0 mg/kg) noticed during March month (Table 5, Fig. 6).

Table 5: Monthly Variations of (Pb) mg/kg in the Soil with Mean in Al-Garraff Oil Field

Locations Month 2022	S-1	S-2	S-3	S-4	S-5	S-6	S-7	S-8	S-9	S-10
March	0.000	0.000	0.000	0.000	0.000	0.000	0.000	0.000	0.000	0.000
April	310.000	317.000	687.890	10.330	289.000	214.000	320.000	308.000	986.890	177.000
May	341.500	350.100	720.140	42.580	321.250	244.470	352.190	341.150	1019.140	209.250
June	371.620	383.220	750.260	71.700	351.370	274.590	382.310	371.270	1021.260	240.370
July	393.210	403.800	770.840	92.300	371.950	295.170	402.400	391.850	1041.840	261.200
August	416.580	427.000	793.340	114.800	394.450	317.240	424.900	414.350	1064.340	284.520
Mean	305.485	313.520	620.412	55.285	288.003	224.245	313.633	304.437	855.578	195.390

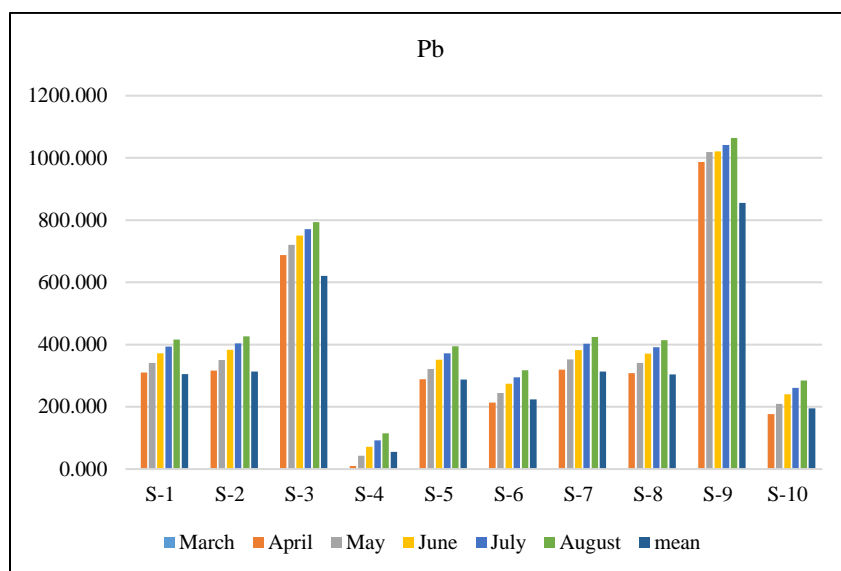


Fig. 6: Monthly Concentrations of (Pb) mg/kg at Al-Garraff Oil Field

Nickel (Ni)

Monthly variations of Nickel (Ni) mg/kg were observed during this study. The highest month concentrations (129.7 mg/kg) detected during August month, while lowest month concentration (51.7 mg/kg) noticed during March month (Table 6, Fig. 7).

Table 6: Monthly Variations of (Ni) mg/kg in the Soil with Mean in Al-Garraff Oil Field

Locations Month 2022	S-1	S-2	S-3	S-4	S-5	S-6	S-7	S-8	S-9	S-10
March	60.920	55.062	51.730	73.860	64.600	59.110	57.220	71.330	76.320	55.300
April	66.200	60.342	57.010	79.140	69.880	64.390	62.500	76.610	81.600	60.580
May	60.920	55.062	51.730	73.860	64.600	59.110	57.220	71.330	76.320	55.300
June	72.000	66.142	62.810	84.870	76.680	70.190	67.300	83.410	87.400	66.380
July	101.000	95.180	91.810	114.200	105.680	100.000	96.300	112.410	117.210	95.380
August	114.100	108.100	104.030	126.420	120.000	112.220	108.520	124.630	129.740	107.600
Mean	79.190	73.315	69.853	92.058	83.573	77.503	74.843	89.953	94.765	73.423

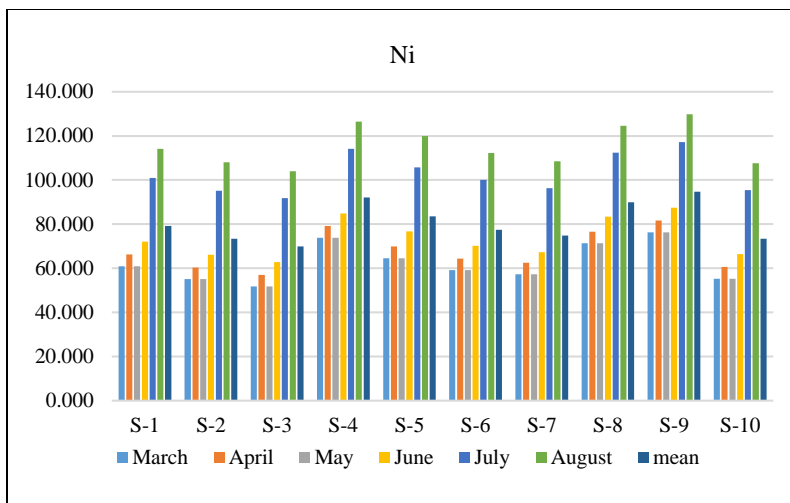


Fig. 7: Monthly Concentrations of (Ni) mg/kg at Al-Garraff Oil Field

Zinc (Zn)

Monthly variations of Zinc (Zn) mg/kg were observed during this study. The highest month concentrations (877.1 mg/kg) detected during August month, while lowest month concentration (65.32 mg/kg) noticed during March month (Table 7, Fig. 8).

Table 7: Monthly Variations of (Zi) mg/kg in the Soil with Mean in Al-Garraff Oil Field

Locations Month 2022	S-1	S-2	S-3	S-4	S-5	S-6	S-7	S-8	S-9	S-10
March	126.000	241.000	98.860	69.830	85.610	79.950	78.520	94.293	251.000	65.320
April	646.000	743.000	618.860	589.830	605.610	599.950	598.520	614.293	731.000	585.320
May	666.500	762.470	639.360	610.330	626.110	620.450	619.020	634.793	751.500	605.820
June	685.200	781.170	658.060	629.030	644.810	639.150	637.720	722.493	725.200	624.520
July	736.050	831.950	709.940	679.880	695.660	690.000	689.050	773.343	776.050	676.100
August	782.110	877.100	754.940	724.880	741.200	735.000	734.050	819.340	821.050	721.100
Mean	606.977	706.115	580.003	550.630	566.500	560.750	559.480	609.759	675.967	546.363

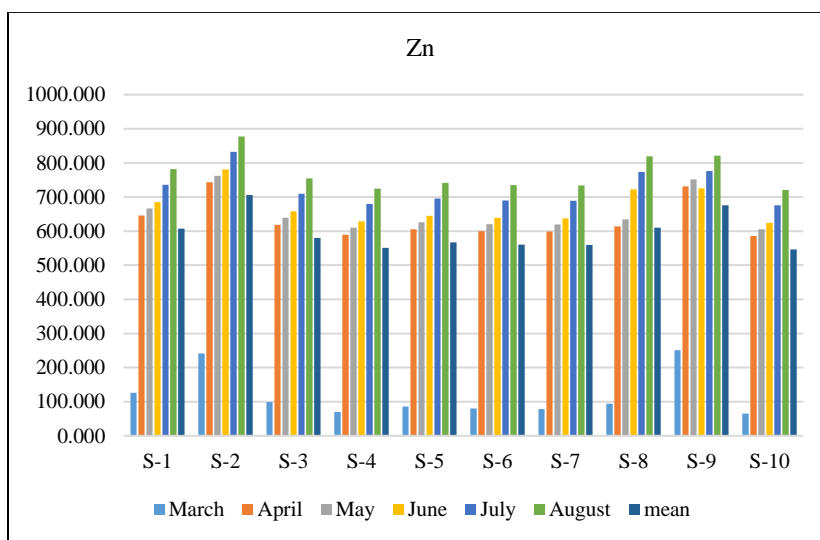


Fig. 8: Monthly Concentrations of (Zi) mg/kg at Al-Garraff Oil Field

Result and Discussion

Indices of Pollution

Various indices, such as the metal enrichment factor (EF), geoaccumulation indices (Igeo), and contamination factor (CF), are typically employed to identify metal concentrations of environmental concern [8]. Usually, these indices are computed using the exchangeable portion of the soil as it accurately represents the fraction of the soil that is available for biological processes. The soil's bio-available metal content has a decisive effect on soil quality and is utilized in food production. Consequently, the evaluation of metal contamination is crucial in agricultural regions close to contamination sources in this study, the pollution assessment in the studied area is performed by calculating the index (Igeo).

Geoaccumulation Index (Igeo)

The geoaccumulation index (Igeo) was also used to evaluate metal contamination in the Garraf Oil Field soil.

The index for geoaccumulation is described as follows:

$$I_{geo} = \log_2 \left(\frac{C_n}{1.5 \cdot B_n} \right) \quad (1)$$

Where C_n is the measured concentration of heavy metal (n) in the soils, B_n is the geochemical background value of element n in the average shale, and 1.5 is the background matrix correction factor due to lithogenic effects.

The index (Igeo) is an expression of the extent of contamination in the soil with heavy metals, and it was used [5], as it relied on the concentration of elements in the earth's crust as a reference concentration for the elements, due to the difficulty of obtaining a reference sample resulting from the increases in human influences on the environment. The soil was classified according to the Geoaccumulation index aggregation as in the Table (8) which represents the classification of soils according to the factor of geochemical aggregation [4].

Table 8: Polluted Level Depending on the Index Geoaccumulation (Igeo)

Class	Value	Scale of Contamination Level
0	$I_{geo} \leq 0$	Uncontaminated
1	$0 < I_{geo} < 1$	Uncontaminated to moderately contaminated
2	$1 \leq I_{geo} < 2$	Moderately contaminated
3	$2 \leq I_{geo} < 3$	Moderately to heavily contaminated
4	$3 \leq I_{geo} < 4$	Heavily contaminated
5	$4 \leq I_{geo} < 5$	Heavily to extremely contaminated
6	$I_{geo} \geq 5$	Extremely contaminated

The results of the geoaccumulation index by applying the Equation (1) that demonstrated in table (9).

Table 9: Result of Geoaccumulation Index (Igeo) in Locations of Study Area

Station	Geoaccumulation Index Igeo						
	Cd	Cr	Mn	Zn	Cu	Pb	Ni
S-1	2.859	0.064	7.467	2.357	-0.799	4.348	-0.770
S-2	2.900	0.001	7.555	2.575	-1.125	4.386	-0.881
S-3	2.860	-0.329	7.105	2.291	-1.255	5.370	-0.951
S-4	2.990	0.182	7.585	2.216	-0.997	1.882	-0.552
S-5	2.691	0.223	7.648	2.257	-1.822	4.263	-0.692
S-6	2.762	0.080	7.610	2.242	-1.154	3.902	-0.801
S-7	2.709	-0.082	7.564	2.239	-1.277	4.386	-0.851
S-8	3.016	0.080	7.523	2.363	-0.841	4.343	-0.586
S-9	2.620	-0.427	7.104	2.512	0.571	5.834	-0.511
S-10	2.474	0.029	7.186	2.205	-1.145	3.703	-0.879
Mean	2.788	-0.018	7.435	2.326	-0.984	4.242	-0.747
Contamination level	Moderately to heavily contaminated	Uncontaminated	Extremely contaminated	Moderately to heavily contaminated	Uncontaminated	Heavily to extremely contaminated	Uncontaminated

The results showed that the highest concentration of the enrichment factor for the element Cadmium (Cd) (3.016) mg/kg dry weight in station No. (8), while the lowest concentration was (2.474) in station No. (10), and the highest concentration of Chromium (Cr) was (0.223) mg/kg dry weight in station No. (5), while the lowest concentration was (-0.427) mg/kg in station No. (9), and the highest concentration of Manganese (Mn) was (7.648) mg/kg dry weight in station No. (5), while the lowest concentration was (7.104) in station No. (9). The highest concentration of Zinc (Zn) was (2.575) mg/kg dry weight in station No. (2), while the lowest concentration was (2.205) in station No. (10). The highest concentration of Copper (Cu) was (0.571) mg/kg in station No. (9) while the lowest concentration was (-1.822) in station No. (5). The highest concentration of lead (Pb) was (5.834) mg/kg in station No. (9) while the lowest concentration was (1.882) in station No. (4). The highest concentration of Nickel (Ni) was (-0.511) mg/kg in station No. (9) while the lowest concentration was (-0.951) in station No. (3).

Through Table (9), it is clear to us an increase in the Geoaccumulation Index (Igeo) for the concentrations of the elements according to the following sequence (manganese, lead, cadmium, zinc, chromium, nickel, copper,) at a rate of (7.435, 4.242, 2.788, 2.326, -0.018, -0.747, -0.984) respectively. The results of the indicator varied according to what is prepared in the table (8), some of them were heavy to extremely contaminated (manganese and lead), and others were Moderate to heavily contaminated, as shown in the element (zinc and cadmium). However, the soil was Uncontaminated with an element (chromium, copper, and nickel).

Correlation Matrix

The outcomes of the correlation analysis conducted between the different types of metals made use of all the raw data Table (1-7) in their entirety. The data on the correlation coefficient are very important to deduce the possible sources of the metals found in the soil samples. According to the findings presented in Table 10, there was a significant correlation between the concentrations of several different metals.

We performed correlation analyses among the metals in Table 10 to examine their shared attributes, such as origin and behaviour, among others. We observed correlations between the metals Cr and Mn. In soil, Cu-Pb, Cu-Ni, Zn-Cu, and Zn-Pb are extremely potent. As a result, there are weak correlations between the metals Cr-Pb, Mn-Pb, Cr-Cu, Mn-Cu, and Cr-Zn. The observed associations among metal concentrations indicate a potential geochemical origin or behaviour that is comparable or identical. The presence of these minerals is facilitated by petroleum residues and the failure to dispose of them properly, as well as the effect of air transport or water transfer to sediments.

Table 10: The Correlation Coefficients of Heavy Metal Concentrations in Al-Garraf Oil Field

	<i>Cd</i>	<i>Cr</i>	<i>Mn</i>	<i>Zn</i>	<i>Cu</i>	<i>Pb</i>	<i>Ni</i>
<i>Cd</i>	1						
<i>Cr</i>	0.264	1					
<i>Mn</i>	0.4051	0.8025	1				
<i>Zn</i>	0.1684	-0.417	-0.174	1			
<i>Cu</i>	-0.218	-0.642	-0.537	0.548	1		
<i>Pb</i>	-0.254	-0.893	-0.696	0.531	0.7329	1	
<i>Ni</i>	0.2311	0.1002	0.1001	0.1578	0.5964	0.1287	1

GIS Interpolation IDW for Soil

The GIS technique was employed to spatially map the distribution of each petroleum component, specifically the hazardous materials (HMs), in soil samples. The IDW technique was utilized to demonstrate the quantitative distribution intensity or interpolate each component across the researched area. The process of interpolating values at unidentified locations by employing known values or sample points [2]. Unfamiliar values can be predicted for any given set of geographical point data. Deterministic interpolation methods are distinguished from geostatistical methods [7]. Deterministic interpolation methods, including Inverse Distance Weighting (IDW), produce a surface through the utilisation of mathematical algorithms or observed data points. Kriging and other geostatistical interpolation methods are founded on statistical principles. On the basis of the degree of similarity, the IDW method is utilised in this investigation to determine the degree of similarity between cells. In this study, the utilisation of this approach is especially beneficial owing to the accessibility of pertinent data. Furthermore, the precision of Inverse Distance Weighted is nearly equivalent to that of other interpolation methods, such as IDW.

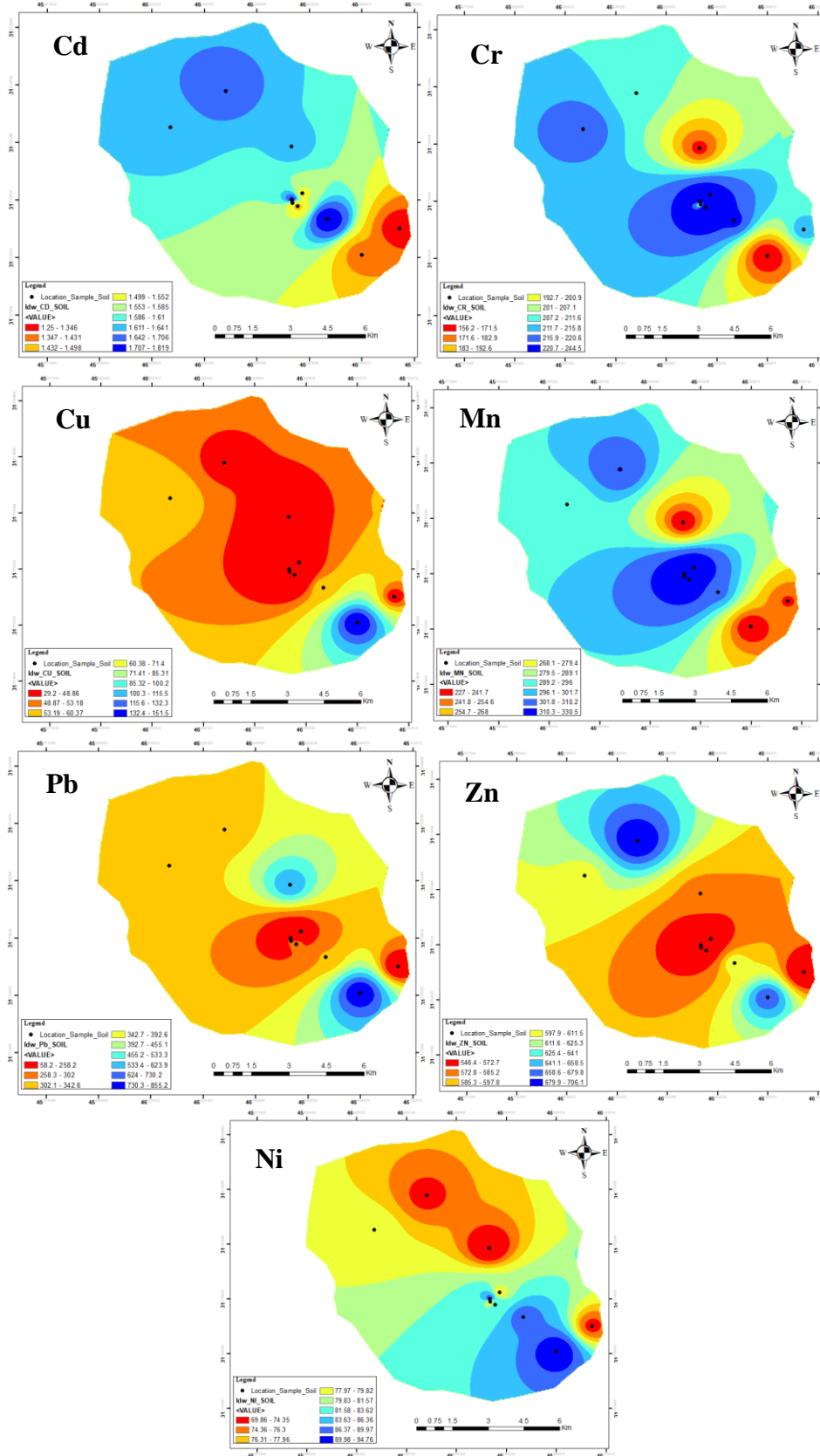


Fig. 9: Spatial Distribution of Parameters in Soil Using IDW Method

The spatial distribution of the elements that were measured in the region under investigation provided a visual representation of the current state of the oil field in terms of the pollution that is caused by oil operations. In this case, Fig. 9 illustrates the normal gradient of the components as well as the extent to which their concentrations are dispersed across the entire research region. The following are the findings that emerged from the analysis: the element (Cd) with the biggest effect in the sample range in (S-2, S-8). When it came to the element (Cr), the samples (S-4, S-5, and S-6) had the most significant impact, whereas the sample (S-9) had the highest concentration of the element (Cu). Because the element (Mn) was found at the maximum concentration in several samples (S-4, S-5, S-6, and S-7), it was found to be more broadly distributed. Particularly evidently, the elements Pb-Ni exhibited the greatest impact on a single (S-9).

Conclusion

The results revealed elevated levels of heavy metal contamination in areas adjacent to the Garraf Oil Field. The Geoaccumulation Index (I_{geo}) values indicated that the soil was unpolluted with Cr, Cu, and Ni; moderately contaminated with the heavy metals Cd and Zn; extremely contaminated with Mn; and heavily to extremely contaminated with Pb metal. The Pearson correlation matrix also shows a strong positive relationship between Cr-Mn, Cu-Pb, Cu-Ni, Zn-Cu, and Zn-Pb. This suggests that these heavy metals may all come from the same place. We investigated the temporal-spatial distribution of these pollutants using GIS in conjunction with inverse distance-weighted interpolation (IDW). The resulting chemical-physical pollution diagrams show that the epicentre of oil activities, especially the areas around the oil wells, is the most important potential source of pollution in the study area.

References

- Al-Khuzai, M.M., & Maulud, K.N.A. (2022). Evaluation of Soil Pollution Levels in Al-Qadisiyah Governorate, Iraq Using Contamination Index and GIS. *Journal of Ecological Engineering*, 23(3), 206–213. <https://doi.org/10.12911/22998993/145478>
- Al Manmi, D.A.M.A., Abdullah, T.O., Al-Jaf, P.M., & Al-Ansari, N. (2019). Soil and groundwater pollution assessment and delineation of intensity risk map in Sulaymaniyah City, NE of Iraq. *Water (Switzerland)*, 11(10). <https://doi.org/10.3390/w11102158>
- Ao, S.I., & International Association of Engineers. (2012). *World Congress on Engineering : WCE 2012 : 4-6 July, 2012, Imperial College London, London, U.K.* Newswood Ltd.
- Barbieri, M. (2016). The Importance of Enrichment Factor (EF) and Geoaccumulation Index (I_{geo}) to Evaluate the Soil Contamination. *Journal of Geology & Geophysics*, 5(1), 1–4. <https://doi.org/10.4172/2381-8719.1000237>
- Basir, Kimijima, S., Sakakibara, M., Pateda, S.M., & Sera, K. (2022). Contamination Level in Geo-Accumulation Index of River Sediments at Artisanal and Small-Scale Gold Mining Area in Gorontalo Province, Indonesia. *International Journal of Environmental Research and Public Health*, 19(10), 6094. <https://doi.org/10.3390/ijerph19106094>
- Boori, M.S., Choudhary, K., Kupriyanov, A., Sugimoto, A., & Evers, M. (2016). Natural and environmental vulnerability analysis through remote sensing and GIS techniques: A case study of Indigirka River basin, Eastern Siberia, Russia. In *Earth Resources and Environmental Remote Sensing/GIS Applications VII, 10005*, 193-202. SPIE. <https://doi.org/10.1117/12.2240917>
- El-Zeiny, A.M., & Elbeih, S.F. (2019). GIS-Based Evaluation of Groundwater Quality and Suitability in Dakhla Oases, Egypt. *Earth Systems and Environment*, 3(3), 507–523. <https://doi.org/10.1007/s41748-019-00112-1>
- Feng, H., Jiang, H., Gao, W., Weinstein, M.P., Zhang, Q., Zhang, W., Yu, L., Yuan, D., & Tao, J. (2011). Metal contamination in sediments of the western Bohai Bay and adjacent estuaries, China. *Journal of Environmental Management*, 92(4), 1185–1197. <https://doi.org/10.1016/j.jenvman.2010.11.020>
- Guo, G., Zhang, D., & Wang, Y. (2021). Characteristics of heavy metals in size-fractionated atmospheric particulate matters and associated health risk assessment based on the respiratory deposition. *Environmental Geochemistry and Health*, 43(1), 285–299. <https://doi.org/10.1007/s10653-020-00706-z>
- Ivars, M.J. (2007). Microwave assisted digestion of sediments, sludges, soils and oils. *Test Methods For Evaluating Solid Waste. Washington DC: US Environmental Protection Agency*, 7(3), 213–221. <https://www.epa.gov/sites/default/files/2015-12/documents/3051a.pdf>
- Ololade, I.A. (2014). An Assessment of Heavy-Metal Contamination in Soils within Auto-Mechanic Workshops Using Enrichment and Contamination Factors with Geoaccumulation Indexes. *Journal of Environmental Protection*, 05(11), 970–982. <https://doi.org/10.4236/jep.2014.511098>

- Qiao, P., Lei, M., Yang, S., Yang, J., Guo, G., & Zhou, X. (2018). Comparing ordinary kriging and inverse distance weighting for soil as pollution in Beijing. *Environmental Science and Pollution Research*, 25(16), 15597–15608. <https://doi.org/10.1007/s11356-018-1552-y>
- Ribes, A., Grimalt, J.O., García, C.J.T., & Cuevas, E. (2003). Polycyclic Aromatic Hydrocarbons in Mountain Soils of the Subtropical Atlantic. *Journal of Environmental Quality*, 32(3), 977–987. <https://doi.org/10.2134/jeq2003.9770>
- Salahalden, V.F., Shareef, M.A., & Al Nuaimy, Q.A.M. (2023). Characterization of the Chemical Properties of Deposited Red Clay Soil Using GIS Based Inverse Distance Weighted Method in Kirkuk City, Iraq. *Ecological Engineering and Environmental Technology*, 24(7), 46–60. <https://doi.org/10.12912/27197050/169571>
- Song, S. (2008). A GIS-based approach to spatio-temporal analysis of urban air quality in Chengdu plain. *International Archives of the Photogrammetry, Remote Sensing and Spatial Information Sciences - ISPRS Archives*, 37(2), 1447–1450.
- Ukhurebor, K.E., Athar, H., Adetunji, C.O., Aigbe, U.O., Onyancha, R.B., & Abifarin, O. (2021). Environmental implications of petroleum spillages in the Niger Delta region of Nigeria: a review. *Journal of Environmental Management*, 293, 112872. <https://doi.org/10.1016/j.jenvman.2021.112872>